CSIRO PUBLISHING
www.publish.csiro.au/journals/ajb *Australian Journal of Botany*, 2011, **59**, 563–574

Histo- and cytopathology of trunk phloem necrosis, a form of rubber tree (*Hevea brasiliensis* Müll. Arg.) tapping panel dryness

Elisabeth de Faÿ

Unité Mixte de Recherche Université Henri Poincaré/Institut National de Recherche Agronomique n°1136, Nancy, France. Email: defaye@scbiol.uhp-nancy.fr

Abstract. Trunk phloem necrosis (TPN) is a physiological disease of rubber tree (*Hevea brasiliensis* Müll. Arg.) discovered in the 1980s. It has been distinguished from rubber tree tapping panel dryness (TPD) by its macroscopic symptoms and presumed origin. But little attention has been paid to its microscopic features, and there is now some evidence that both syndromes could be linked to an impaired cyanide metabolism. In order to characterise TPN and compare it with TPD microscopically, the inner phloem of tapping panels was investigated by light and transmission electron microscopy in healthy trees and TPN-affected trees. TPN-affected phloem presented numerous and varied structural and ultrastructural features. There were signs of cellular deterioration in a great number of specialised cells, i.e. laticifers and sieve tubes, and not very specialised cells, i.e. parenchyma cells and companion cells. There were also signs of cellular dedifferentiation in other parenchymatous cells, e.g. in tylosoids and hyperplasic cells. These cells were derived from parenchyma cells that ensheath laticifers in which the latex coagulated. Numerous structural features of TPN are common to TPD, notably tylosoids associated with *in situ* coagulated latex, which are also known to be early structural markers of TPD and cyanide-induced. It is therefore concluded that TPN is identical to or a variant of TPD, and is a degenerative disease of rubber tree trunk phloem resembling plant stress response, programmed cell death and plant tumourigenesis in some aspects.

Introduction

Rubber tree (*Hevea brasiliensis* Müll. Arg.) is an important industrial crop, natural rubber representing almost half of the total world rubber production (42% in 2005). As in other crops, various plant physiological conditions and pathogenic diseases influence rubber production. The tapping panel dryness (TPD) is one of the most serious threats to natural rubber production. It is estimated that TPD contributes to 15–20% loss of the annual rubber production, with an incidence of 20–50% of productive trees affected by TPD, in almost all rubber-growing regions. TPD is an issue very specific to rubber tree, resulting in the cessation of latex flow (bark dryness) and a reduction of the tapping stand. It is now admitted that TPD is a physiological disorder resulting from abiotic stress, with two forms: on the one hand, a reversible tapping cut dryness without any visible sign of bark necrosis, and on the other hand, an irreversible bark necrosis or brown bast (Jacob *et al*. 1994). Attention was first drawn, as soon as the beginning of the 20th century, by browning of the inner part of tapping panels (barks of the exploited side of trunks), its necrosis and progressive destructuration. So the phenomenon was first called brown bast (Bobilioff 1919). But the development of a simple tapping cut dryness without any sign of browning, i.e. appearance of dry zones (without latex dripping out) along the tapping cut, was also observed on many trees and could be very extensive in severe cases. According to Clément-Demange *et al*. (2007), there is uncertainty about the relationships between the two forms. Indeed, some researchers assume that TPD is directly linked to over-exploitation (excessive tapping and intense ethylene stimulation), and that there is a progressive evolution from tapping cut dryness (reversible TPD) to brown bast (irreversible TPD), whereas others think that they are two distinct diseases differing in their origin.

A syndrome with browning and necrosis of the trunk bark was discovered in the 1980s in rubber trees of West African plantations and seen again in most modern rubber plantations worldwide, with a wide range of severity across sites. Trunk phloem necrosis (TPN), also termed bark necrosis (Nandris *et al*. 1991), has been distinguished from TPD by the extent of browning (presence of deep brown sheets) and necrosis (presence of superficial necrotic patches) and by their main location at the base of the trunk near the scion/rootstock junction (Nandris *et al*. 2004). Because this syndrome was sometimes observed on untapped or newly opened trees, it has been suspected to be favoured by other factors than over-exploitation. An ecophysiological study has suggested that TPN was favoured by some environmental factors, such as high soil compaction (Nandris *et al*. 2004). Biochemical and gene expression studies have suggested that impaired cyanide metabolism might be at the origin of TPN, or at least of its spread within the tree (Chrestin *et al*. 2004). However, it was recently shown in Brazilian clones differently sensitive to TPD that the structural abnormalities specific to irreversible TPD, i.e. tylosoids

 10.1071/BT11070 0067-1924/11/060563

(kinds of tyloses formed in laticifers) associated with *in situ* coagulated latex (de Faÿ and Hébant 1980; de Faÿ 1981; de Faÿ and Jacob 1989), are cyanide-induced (de Faÿ *et al*. 2010). TPD and TPN might thus have the same immediate cause. But it is not yet known if they have the same histological characteristics. Moreover, the fine structural changes that occur within phloem cells with the development of both syndromes had been poorly investigated, particularly at the onset of the disorder.

The present study aims to compare TPN with irreversible TPD and to identify the fine structural changes occurring in young phloem cells of tapping panels when the syndrome was spreading within the trees. It is to examine the bark and specifically the inner phloem of tapping panels by light and transmission electron microscopy (TEM), in healthy and TPN-affected rubber trees.

Materials and methods

Plant material

Plant material was obtained from mature trees of two clones prone to TPN and widely planted in West Africa; those came from plantations located in the same climatic region along the West African coast, with a maximum distance of 250 km from one another. The clone GT1 was selected because TPN had been discovered notably in this clone, and its discoverers provided some specimens in which ultrastructural characterisation of the disease had begun (Nicole *et al*. 1991, 1992) but had needed to be continued. The clone PB 260 was selected because it proved to be the most highly susceptible to TPN in West Africa (GT1 was then classed as fairly susceptible). A total of 10 TPN-affected and three healthy individuals were sampled in three series (Table 1). The number of healthy trees sampled was minimised in each series because the normal histology and cytology of rubber tree had already been examined, notably in GT1 (de Faÿ and Hébant 1980; Hébant and de Faÿ 1980; de Faÿ 1981; de Faÿ *et al*. 1989). Moreover in the literature, there is no suggestion of qualitative anatomical difference between rubber clones selected for their latex yield (case of GT1 and PB 260). The observations from the three controls could be justifiably combined. The trees were identified as healthy or diseased after examining the bark lightly scrapped from the level of tapping panel down to the trunk base, collar and superficial roots, plus the tapping cut and eventually vertical grooves cut in the bark.

Barks were sampled at various levels of the tapping panels, from two or more (up to nine) places per tree; as for the TPN-affected trees: from dry barks and generally at the level of the brown sheets, more rarely at that of necrotic patches, occasionally from non-dry barks or from the front area where latex flow was slowing down; as for healthy trees: under the tapping cut. The sampling places were always more than 20 cm away from one another, and the samples comprising periderm and phloem as deep as to the cambium were taken with a 1–3-cm diameter punch.

Histological methods

For light microscopic examination, samples were immediately immersed in Craf I solution (Sass 1958) prepared at the time of use and in which they can be preserved until sectioning. Later, every sample was cut with a razor blade according to the three directions, transversal, radial axial and tangential axial, so that a well oriented central cuboid was kept. Generally, the outer part, i.e. the hard bark very rich in stone cells (sclereids) and poor in laticifer rings, was also discarded. Then, cross-sections were made with a freezing microtome. Every sample of sectioned soft bark (inner part of the secondary phloem) was systematically treated with 1% Alcian blue in 1% acetic acid to stain the acidic polysaccharides of phloem primary walls blue and with 1% Oil Red O in 90% isopropyl alcohol to stain latex red. Some sections were treated with phloroglucinol-HCl, which specifically stained the cinnamaldehyde groups present in lignins dark pink (Vallet *et al*. 1996). In addition, semi-thin sections obtained from samples fixed and embedded for TEM were stained with a 10-time diluted solution of 1% Toluidine blue in 1% Borax, eventually followed by a post-treatment with I_2/KI solution. Others were pre-treated with 1% periodic acid before staining with 0.5% Toluidine blue in 2.5% Na_2CO_3. Sections of soft bark were observed with a Nikon Optiphot 2 (Nikon Corporation, Tokyo, Japan), usually under white light, occasionally under blue light using a B_2 filter combination (Excitation, 450–500 nm; Emission, 520 nm).

Cytological methods

For TEM examination, samples were treated as follows. Before sampling, small amounts of the fixative 4% p-paraformaldehyde, 0.2% glutaraldehyde in 0.1-M phosphate buffer, pH 7.2, were injected deep into the bark in three points in relation to the future place of sampling: 1–2 cm above, on the right and on the left. After a few minutes, a 1-cm-diameter sample was taken and immediately immersed into some fresh fixative. As soon as possible, the hard bark and eventually the brown sheet were removed, as well as the lateral parts of the samples, in order to save a cuboid of inner soft bark having transversal, radial axial and tangential axial faces. This one was cut into several radial axial slices, themselves cut again into two or three smaller segments elongated axially (sides: 1 mm, length: 5 mm). All these slivers were put into some fresh fixative for ~3 h at 18°C. In total, the

Table 1. Number and health status of the rubber trees used for characterising Trunk phloem necrosis at the structural and ultrastructural levels, and their origin

Number and health status	Clones	Years of sampling	Plantations
Two diseased[A] One healthy[A]	GT 1	1986	SOGB (Société des caoutchoucs de Grand-Béréby), RCI (The Ivory Coast)
Five diseased One healthy	PB 260	2003	SAPH (Société Africaine de plantation d'Hévéas)-SOGB, RCI
Three diseased One healthy	PB 260	2005	GREL (Ghana Rubber Estates Limited), Ghana

[A]Samples previously examined by Nicole *et al*. (1991).

phloem tissues will have been fixed 4 h. After several rinses in 0.1-M phosphate buffer, pH 7.2, the slivers were post-fixed 1 h at 18°C in 1% osmium tetroxide, pH 7.2. Following a further rinse in the phosphate buffer, they were dehydrated in a gradual ethanol series from 25 to 100%, embedded in Durcupan ACM Epoxy. Slivers having largely opened sieve elements (conducting phloem) indicating some of the innermost phloem layers were selected and cut with a RCM ultramicrotome Model MT-7 (RCM Company, Tucson, AZ, USA). Ultrathin transverse sections were contrasted 20 min in uranyl acetate and 20 or 15 min in lead citrate before examination under a Zeiss Microscope Model EM 90 2A (Carl Zeiss AG, Oberkochen, Germany). Staining time was reduced to 15 min for TPN-affected specimens for avoiding excessive contrast.

Results

Structural characteristics of the inner bark of TPN-affected trees

In control trees of the two clones studied, the tapping panels presented the following histology (Fig. 1). It was thick, in the range of 7–10 mm, but laticifers were abundant only in the inner third part (soft bark) (Fig. 1*a*). Laticifers (Fig. 1*a–f*) were arranged in numerous concentric rows called laticifer rings (Fig. 1*a*) typical of the secondary phloem. Adjacent laticifers were anastomosed laterally (Fig. 1*c, d, f*), and their content had a granular aspect (Fig. 1*c, d, f*) indicating the presence of globular structures, principally rubber particles (Fig. 1*f*). The secondary phloem also contained sieve tubes, but the largely opened and apparently empty sieve elements (Fig. 1*b, c*) formed a narrow band (0.2–0.8 mm) adjacent to the cambium (Fig. 1*b*) called conducting phloem. The sieve elements were progressively crushed outwards (Fig. 1*b, c*) and then formed the non-conducting phloem. The other secondary phloem cells (Fig. 1*b–f*) were either companion cells, radial parenchyma cells of vascular rays or axial parenchyma cells including those forming the sheath of laticifer rings (Fig. 1*c, d, f*). A few parenchyma cells turned into tannin cells (Fig. 1*b, d, e*); in places, some others turned into sclereids (stone cells), which progressively formed nodules (Fig. 1*d, e*).

Soft bark of the tapping panel of TPN-affected trees was distinguished from that of healthy trees by several histological or histochemical features, the same in the two clones (Fig. 2). In most laticifers (except generally in the innermost laticifer rings), the latex did not any more appear granular but looked smooth (Fig. 2*a, d, k*) or heterogeneous (Fig. 2*b, c, l*) according to the fixation and staining techniques used. The smooth appearance of the latex following the staining of lipidic material reflected the fusion of rubber globules, which is commonly expressed by *in situ* coagulation of latex. The heterogeneous appearance following Toluidine blue-I_2/KI staining reflected the occurrence of other changes in the laticifer protoplasm. Laticifers having coagulated latex were often invaded by outgrowths of the associated parenchyma cells (laticifer sheath cells) called tylosoids (Fig. 2*d, e*). More outwards, a sort of hyperplasic tissue developed. It consisted of irregularly shaped and arranged parenchymatous cells (Fig. 2*e–g*) presenting peculiar-shaped structures (Fig. 2*f*) and generally a disproportionately large nucleus with prominent nucleoli (data shown below). It resulted from tylosoid proliferation, as shown by the remnants of coagulated latex in the intercellular spaces (Fig. 2*e, g*). It was clear that laticifers were destroyed and dismantled in these places. Wound gum-like golden material (Fig. 2*h*) was positively reactive

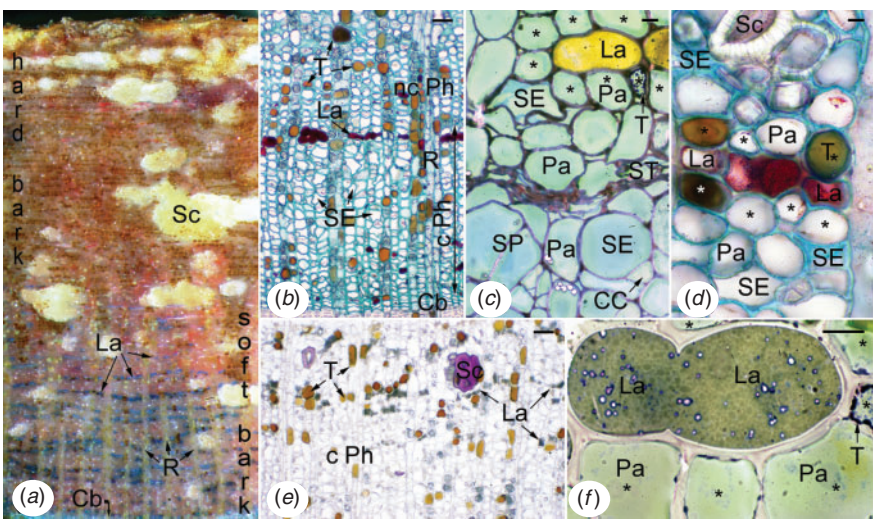

Fig. 1. Normal structure of the trunk bark and secondary phloem of rubber trees (tapping panel of healthy mature trees) belonging to the clones GT1 (*c*, *e*) and PB 260 (*a*, *b*, *d*, *f*). (*a*) Whole bark showing numerous laticifer rings in the inner part. (*b*) View of the secondary phloem close to the cambium showing the conducting phloem. (*c*) Detail of the sieve elements at the boundary between the conducting and the non-conducting phloem. (*d*) Detail of the non-conducting phloem showing a portion of laticifer ring ensheathed by parenchyma cells. (*e*) View of the inner secondary phloem showing the thick lignified walls of rare sclereids starting to form nodules. (*f*) Detail of two anastomosed laticifers and their parenchyma sheath; latex shows numerous rubber particles as green-grey globules and a few particles having blue edge, probably lutoids. Asterisks mark the parenchyma cells ensheathing the laticifers. Cb, cambium; CC, companion cell; c Ph, conducting phloem; nc Ph, non-conducting phloem; La, laticifer; Pa, parenchyma cell; R, ray cell; Sc, sclereid; SE, sieve element; SP, sieve plate; T, tannin cell. Bars, 50 µm (*a*, *b*, *e*), 10 µm (*c*, *d*, *f*). Transversal sections (*c*, *f* semi-thin ones) stained with Alcian blue-Oil Red O and rapidly treated with ethanol 70 (*a*); only stained with Alcian blue-Oil Red O (*b* and *d*); stained with Toluidine blue followed by I_2/IK (*c* and *f*); stained with phloroglucinol-HCl (*e*).

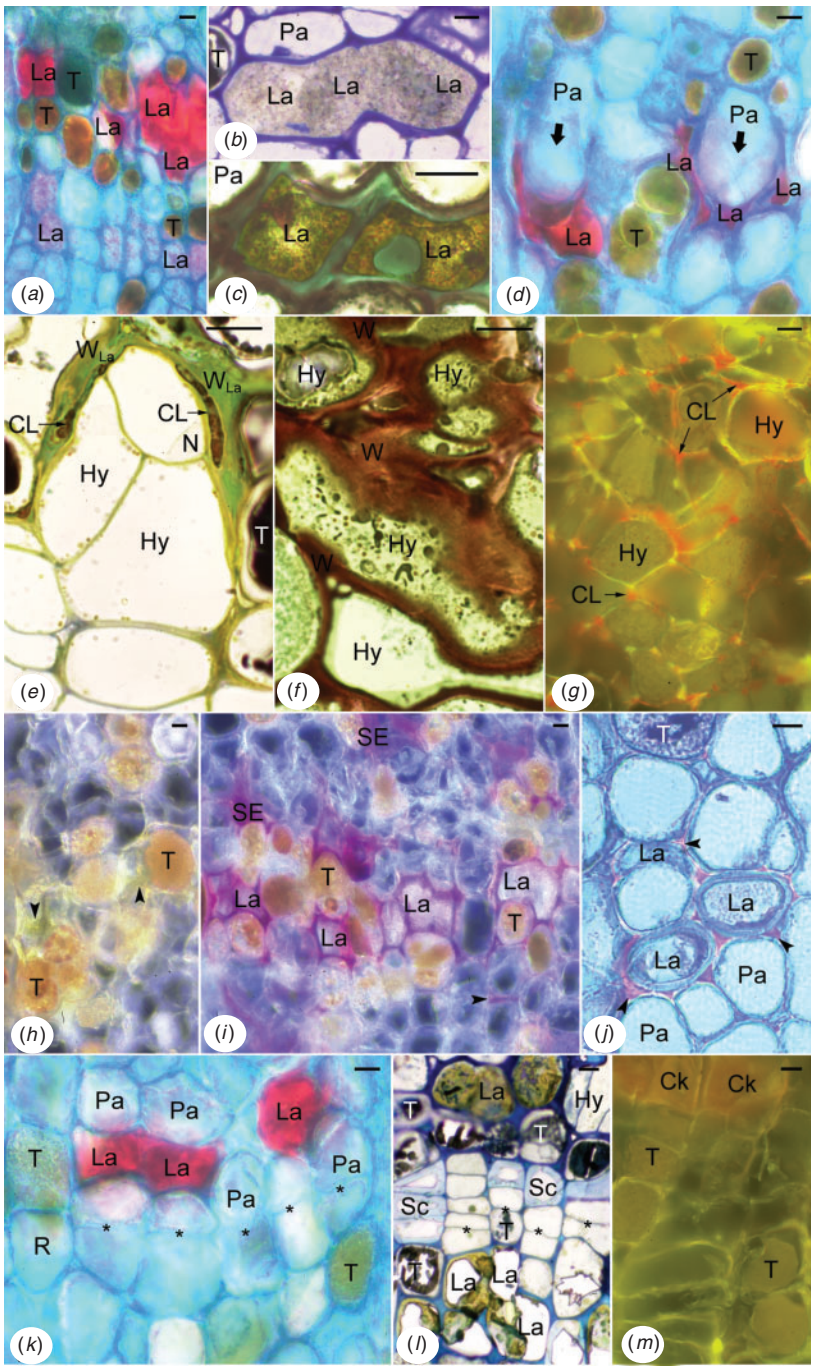

Fig. 2. Tapping panel secondary phloem of Trunk phloem necrosis-affected heveas of the clones GT1 (*a*, *d*, *e*, *i–k*) and PB 260 (*b*, *c*, *f–h*, *l*, *m*) showing varied structural changes. (*a*) Two rings of laticifers, the outer with non-granular (coagulated) latex, the inner with granular latex. (*b*) Three anastomosed laticifers whose rubber particles start to coalesce in the middle. (*c*) Two laticifers, which have the content stained heterogeneously. (*d*) Laticifers invaded by cell outgrowths (large arrows) from parenchyma sheath of the laticifers (formation of tylosoids). (*e*) Hyperplasic cells developed after invasion of a laticifer. See the coagulated latex flattened between the thick laticifer wall and the thin walls of the hyperplasic cells. (*f*) Hyperplasic cells of varied size, shape and orientation, the content of which is more or less dense. (*g*) Coagulated latex stretched in the intercellular spaces of hyperplasic cells (small arrows). (*h*) Golden yellow deposits onto intra- and intercellular spaces (arrowheads). (*i*) Lignified materials at the level of laticifers, sieve elements and intercellular spaces (arrowhead). (*j*) Wall alteration starting at the level of middle lamellae and intercellular spaces, particularly next to three laticifers. (*k*) Additional meristematic layer that has just arose from a laticifer sheath. (*l*) Additional meristematic layer, which has functioned and formed some sclereids. (*m*) Three new radial files of cells, which have differentiated cork cells (upper side). Asterisks mark new walls. CL, coagulated latex; Ck, cork cell; Hy, hyperplasic cell; La, laticifer; N, nucleus; Pa, parenchyma cell; R, ray cell; Sc, sclereid (stone cell); SE, sieve element; T, tannin cell; W, wall. Bars: 10 µm. Transversal sections (*b*, *c*, *e*, *f*, *j*, *l*, semi-thin ones) stained with Alcian blue-Oil Red O (*a*, *d*, *k*); stained with Toluidine blue alone (*b*) followed by I_2/IK (*c*, *e*, *f*, *l*) or preceded by treatment with periodic acid (*j*); stained with Oil Red O but viewed under blue light (*g*, *m*); non-stained (*h*); stained with phloroglucinol-HCl (*i*).

to phloroglucinol-HCL (Fig. 2*i*). It impregnated the walls of numerous laticifers, crushed sieve elements and sometimes parenchyma cells, and spread into the intra- and intercellular spaces (Fig. 2*h–j*). First changes occurred at the level of the middle lamella and intercellular spaces between laticifers and parenchyma cells of the laticifer sheath (Fig. 2*j*). In other places, more or less small tertiary formations were found around parts of laticifer rings having coagulated latex (Fig. 2*k*, *l*). They came from additional meristematic layers arising in the parenchyma sheath of laticifers (Fig. 2*k*), or in the vicinity when the sheath was rich in tannins (Fig. 2*l*). They produced parenchymatous cells, which generally differentiated themselves in tannin cells (Fig. 2*l*, *m*), stone cells (Fig. 2*l*), or eventually cork cells (Fig. 2*m*). Tannins were always abundant (Fig. 2*a*, *b*, *d*, *e*, *h–m*), but these and the wound gum-like secretions accumulated strongly at the level of brown sheets and necrotic patches.

Distribution and amount of each type of abnormality varied greatly between and within diseased trees, but tylosoids and/or hyperplasic tissue were always present at the level of brown sheets and necrotic patches as well as in deeper layers (Fig. 3). However, they could also be found around these areas in zones of normal-coloured bark, sometimes in abundance (Fig. 3).

Ultrastructural characteristics of the young phloem of TPN-affected trees

In control trees of both clones (exploited mature trees), and more precisely in the inner secondary phloem of tapping panels, the cells presented the following features (Fig. 4). Laticifers were generally filled up with rubber particles of various sizes and

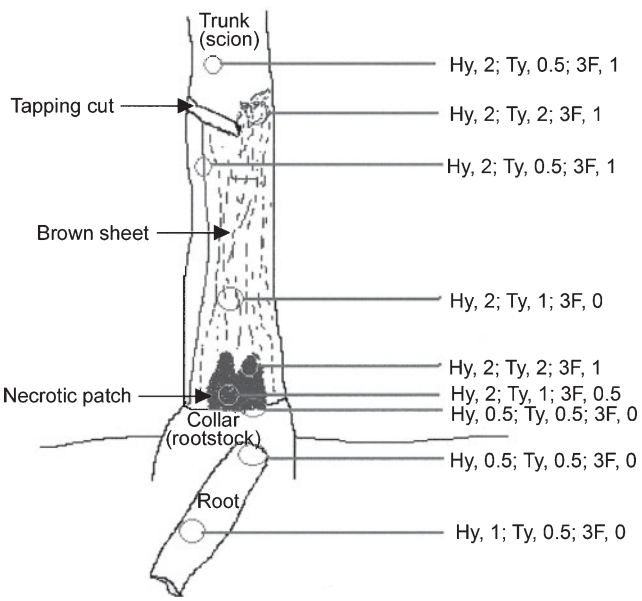

Fig. 3. Presence and abundance of hyperplasic cells, tylosoids and tertiary formations according to the place of bark sampling in a mature hevea suffering from Trunk phloem necrosis (clone PB 260): at the level of necrotic patch and brown sheet, at the interface brown sheet/bark without browning, above the tapping cut, at the interface scion/rootstock and in a root. Abbreviations and symbols: Hy, hyperplasic cells; Ty, tylosoids; 3F, tertiary formations; 2, numerous; 1, few; 0.5, rare; 0, absent.

presented a few organelles (Fig. 4*a*). Small mitochondria flattened against the cell walls were the most frequent (Fig. 4*a*, *c*); other ultrastructures were only found in places or were very rare, such as nucleus (Fig. 4*b*). Mature sieve elements (dilated large elements, Fig. 4*d*, *g*) showed sieve plates with typical linings of callose-like substance and masses of P-protein fibrils into and around the pores (Fig. 4*d*). Starch-plastids (Fig. 4*d*, *f*) and stacks of endoplasmic reticulum (ER) parallel to and associated with the plasma membranes (Fig. 4*d–f*) were numerous; rare mitochondria were found in the parietal cytoplasm (Fig. 4*e*). Crushed sieve elements of the non-conducting phloem did not any more contain recognisable organelles or membrane systems (Fig. 4*v*). Recognisable from their pore plasmodesmal units incorporating fine linings of callose-like substance in the common wall with the sieve elements (Fig. 4*k*), companion cells displayed a more or less electron-lucent cytoplasm and small membrane-bound cavities, i.e. vacuoles or other vesicles (Fig. 4*g–l*, centre). But some of them also presented features indicating a more advanced stage of development: often rather flocculent nucleoplasm (Fig. 4*l*), sometimes membrane breakage at the level of the nuclear envelope (Fig. 4*l*) and cavities containing osmiophilic material close to the plasma membranes (Fig. 4*j*). Like companion cells, a part of the parenchyma cells, i.e. the axial ones including the laticifer sheath cells, showed electron-lucent cytoplasm and organelles, and several membrane-bound cavities (Fig. 4*m*, *s–v*). The other parenchyma cells, i.e. the radial ones, displayed electron-dense cytoplasm and organelles, and a large central vacuole (Fig. 4*g*, *m–r*, *v*). Both kinds of cells could be adjacent and symplastically connected (Fig. 4*g*, *m*, *t*, *v*). The rare tanniferous cells had often an electron-dense cytoplasm and presented not much electron-opaque tannins (Fig. 4*t*, *u*, top) in their large central vacuole. In all the parenchyma cells, plasmalemma and internal membranes (Fig. 4*g–v*) appeared to be normal even in the non-conducting phloem, as well as plasmodesmata (Fig. 4*k*, *q*, *r*, *t*). All the cell walls were fairly electron-dense (Fig. 4*a–v*) but with the middle lamella denser, especially in the cell corners (Fig. 4*g*, *m*, *n*). It was the same in the non-conducting phloem, even for the deformed walls of the crushed sieve elements (Fig. 4*v*).

Inner secondary phloem of the tapping panel of TPN-affected trees was distinguished from that of healthy trees by many ultrastructural abnormalities in all the cellular types (Fig. 5), even very close to the cambium. Most laticifers contained fused rubber particles mixed with very electron-opaque material and sometimes electron-translucent remnants of unrecognisable structures (Fig. 5*a*, *b*). Some laticifers also contained a parenchymatous cell that had a non-straight thin wall apparently pliable (Fig. 5*b*) revealing the budding at the origin of the tylosoid. In phloem layers closer to the cambium and in the dry/non-dry intermediate region of the trunk (front area), laticifers showed rounded rubber particles but with tiny electron-opaque granules lying at their surface (Fig. 5*c*). The osmiophilic material was deposited in mass onto the plasma membrane (Fig. 5*c*). Most sieve elements accumulated electron-opaque material in the non-conducting phloem (crushed sieve elements) and also in some non-crushed sieve elements closer to the cambium, even in the dry/non-dry front area (Fig. 5*d*, *e*). In the latter case, it was mainly found around the sieve plates that had an altered structure (Fig. 5*d*, *e*). Moreover, in all the non-crushed sieve elements,

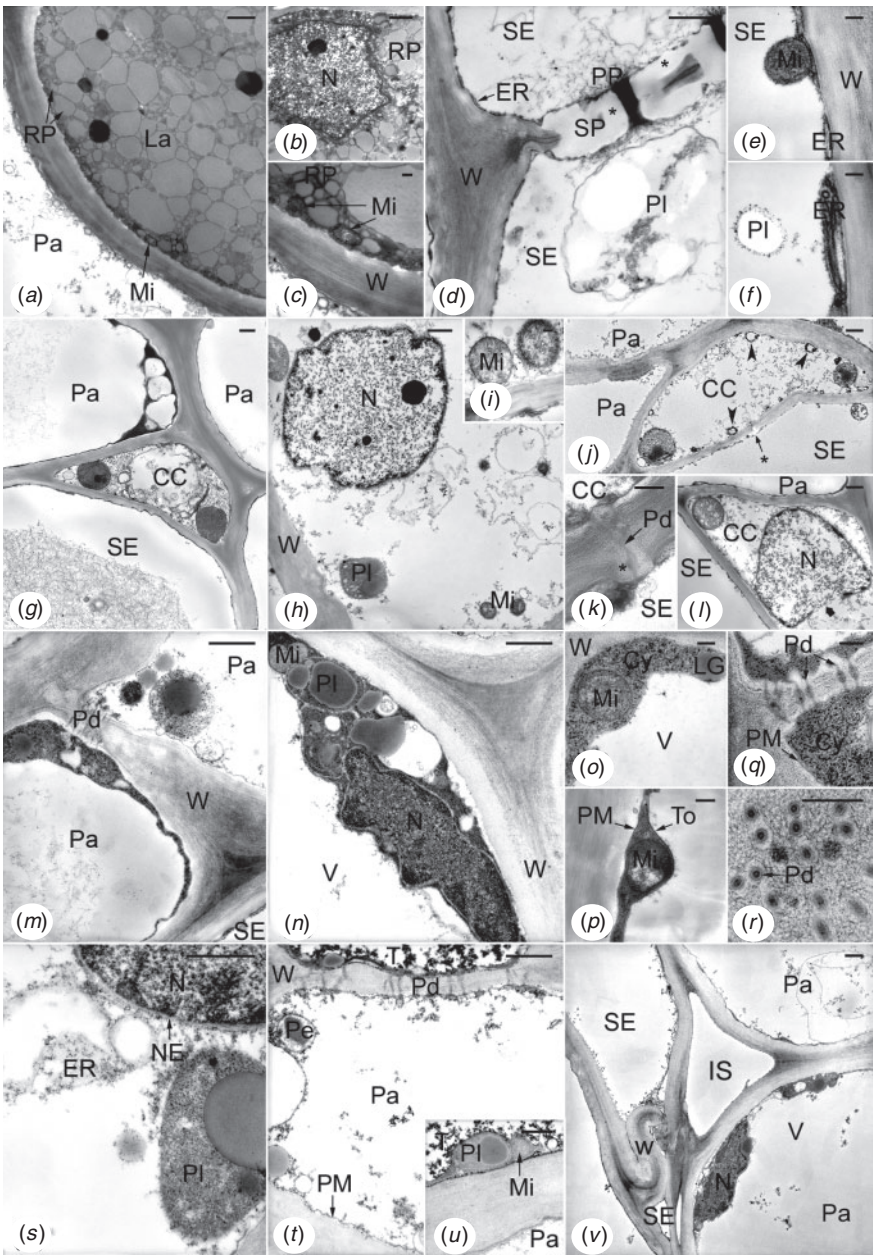

Fig. 4. Ultrastructure of the tapping panel inner secondary phloem of healthy hevea trees (exploited mature trees) belonging to the clones GT1 (*a*, *c*, *e*, *f*, *h*, *j–m*, *p*, *r*, *t–v*) and PB 260 (*b*, *d*, *g*, *i*, *n*, *o*, *q*, *s*). (*a–c*) View showing a laticifer and details. Note that the globular large- and medium-sized rubber particles were here distorted due to crowding. (*d–f*) View showing details of sieve elements. (*g*) View of conducting phloem showing notably a companion cell having a fairly electron-lucent ('clear') cytoplasm and a parenchyma cell having an electron-dense cytoplasm (top left). (*h*, *i*) Detail of a companion cell having a 'clear' cytoplasm. (*j*) Phloem showing a 'clear' companion cell having vesicles containing osmiophilic material close to the plasmalemma (arrowheads). (*k*) Pore plasmodesmal unit. (*l*) Phloem showing a companion cell having the nuclear envelope broken (large arrow). (*m*) Two kinds of parenchyma cells connected by plasmodesmata. (*n–r*) Details of 'dense' parenchyma cells. (*s*) Detail of a 'clear' parenchyma cell. (*t*, *u*) Other details of such a cell connected to a tannin cell (top). (*v*) Non-conducting phloem recognisable from the deformed walls of crushed sieve elements. Asterisks mark the callose. CC, companion cell; Cy, cytoplasm; ER, endoplasmic reticulum; IS, intercellular space; Mi, mitochondrion; N, nucleus; La, laticifer; LG, lipid globule; NE, nuclear envelope; Pa, parenchyma cell; Pd, plasmodesma; Pe, peroxisome; PF, pit field; Pl, plastid (S-plastid); PM, plasma membrane; PP, P-proteins; RP, rubber particle; SE, sieve element; SP, sieve plate; To, tonoplast; V, vacuole; W, wall. Bars, 1 µm (*a–j*, *l–p*, *s–v*), 0.2 µm (*k*, *q*, *r*). Transversal ultrathin sections stained with uranyl acetate and lead citrate.

the stacks of ER were generally dilated (Fig. 5*d*, *f*); no starch-plastid was recognisable; more or less big masses of callose-like non-osmiophilic material were deposited onto and into the wall common with the companion cell (Fig. 5*d*, *f*).

The other cells, parenchymatous in nature, presented the most varied ultrastructural abnormalities, which could be different according to the origin and location of the cells (Fig. 5*g–s*). The most remarkable cells (Fig. 5*g–l*) were very rich in organelles

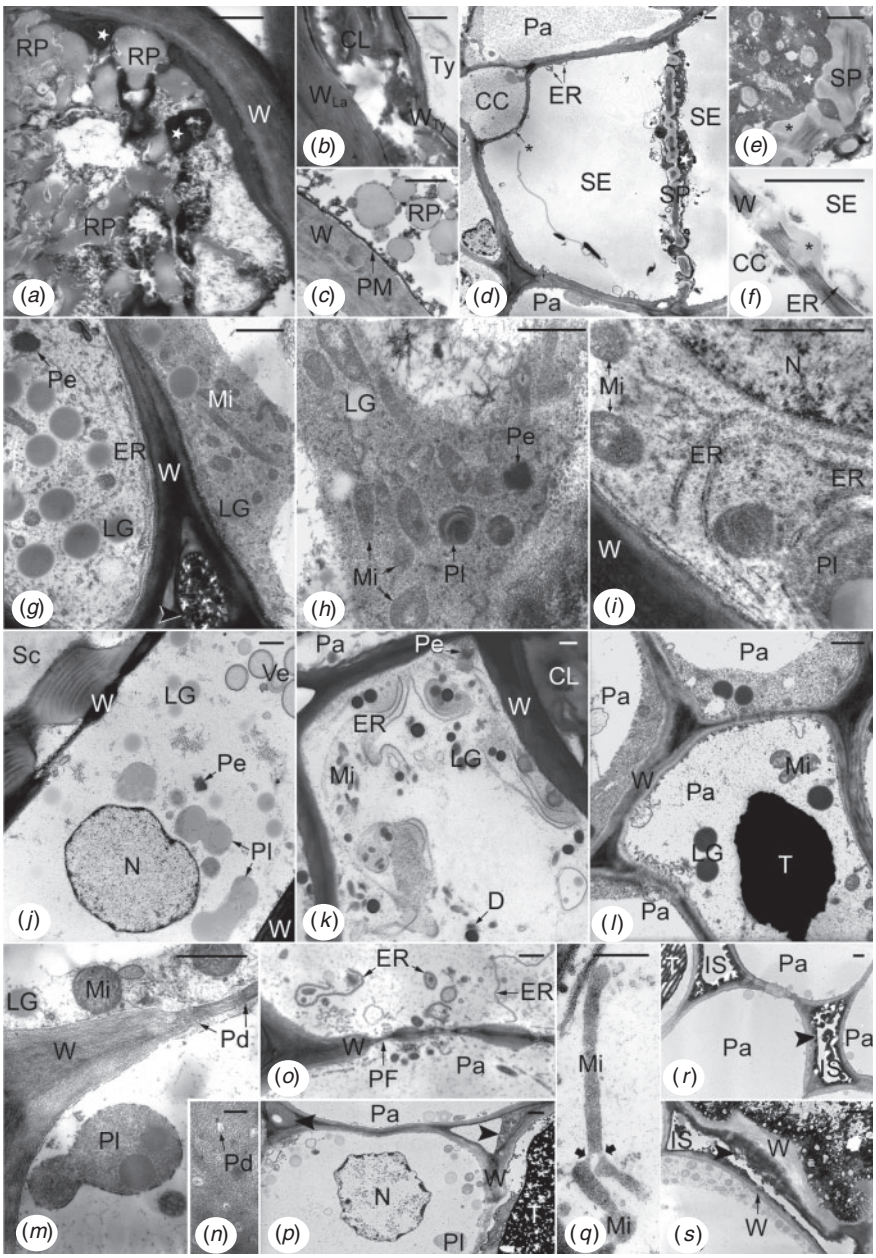

Fig. 5. Ultrastructural changes in the tapping panel inner secondary phloem of Trunk phloem necrosis-affected hevea trees belonging to the clones GT1 (*b*, *i*, *j*, *l*, *q*) and PB 260 (*a*, *c–h*, *k*, *m–p*, *r*, *s*). (*a–c*) Views of laticifers showing various abnormalities. (*d–f*) Views of sieve elements and companion cells showing several abnormalities. (*g–l*) Views of parenchymatous cells displaying signs of dedifferentiation (hyperplasic cells). (*m–s*) Views of phloem parenchyma cells displaying signs of degradation or alteration. Asterisks mark callose-like material; arrowheads mark varied material in the intercellular spaces; white stars mark osmiophilic material in the protoplasm. CC, companion cell; CL, coagulated latex; D, dictyosome; ER, endoplasmic reticulum; IS, intercellular space; La, laticifer; LG, lipid globule; Mi, mitochondrion; N, nucleus; Pa, parenchyma cell; Pd, plasmodesma; Pe, peroxysome; PF, primary pit field; Pl, plastid; PM, plasma membrane; RP, rubber particle; Sc, sclereid; SE, sieve element; SP, sieve plate; T, tannins; Ty, tylosoid; Ve, vesicle; W, wall. Bars, 1 µm (*a–m*, *o–s*), 0.2 µm (*n*). Transversal ultrathin sections stained with uranyl acetate and lead citrate.

plastids and mitochondria, in big lipid globules and in rough ER. The flat ER cisternae were arranged in more or less long and parallel profiles (Fig. 5*g*, *i*, *k*); in some cells, they tended to coil up round organelles or lipid globules (Fig. 5*i*, *k*). The plastids and particularly the mitochondria were elongated and constricted (Fig. 5*g*, *h*, *j*, *k*); their stroma and matrix were generally electron-dense (Fig. 5*g–i*, *j*, *l*). Crystals of peroxisomes were also electron-dense (Fig. 5*g*, *h*, *k*, *j*). The cytoplasm was more or less electron-dense and rich in ribosomes, and the lipid globules were more or less osmiophilic according to the cells (Fig. 5*g–l*). Membrane-bound cavities of different sizes and contents were found in the cytoplasm and periplasm (Fig. 5*h*, *j–l*). There were also electron-translucent large areas containing fibrillar or vesicular materials that were not enclosed by membranes

(Fig. 5*g*, *h*). Nuclei, usually large, exhibited big nucleoli, had a central position, a rounded shape and a normal ultrastructure (Fig. 5*i*, *j*). In the outer part of this abnormal tissue, the cells might exhibit a more or less large central cavity containing densely stained materials (Fig. 5*l*) resembling tannins. Because these parenchymatous cells were always found in the non-conducting phloem layers containing altered and/or dismantled laticifers, they were either hyperplasic cells or cells of tertiary formations depending on if they were issued from budding then proliferation of secondary parenchyma cells or from proliferation alone, respectively.

The other abnormal cells of parenchymatous nature were distinguished particularly by alterations of their membrane systems. Plasma membranes were broken into small pieces (Fig. 5*m*). Outer membranes of mitochondrial, plastidial (Fig. 5*m*, *q*) and nuclear envelopes disappeared up. Tonoplasts were generally not discernible (Fig. 5*m*, *o*, *p*). Plasmodesmata were altered and often empty (Fig. 5*m*, *n*). ER-derived structures containing part of cytoplasm and organelles or unrecognisable materials were abundant (Fig. 5*o*). Moreover, cytoplasm and nucleoplasm tended to be very translucent and flocculent (Fig. 5*m*, *o–q*), but heterochromatin was condensed at the periphery of the nucleus (Fig. 5*p*). Mitochondria and plastids also tended to be electron-transparent. However, in some cells, mitochondria and plastids could be giant and branched (Fig. 5*q*). In other cells, lipid globules and tannins were extremely electron-dense. All these features were grouped together in the inner phloem layers below the brown sheets, but closer to the cambium than the first kind of abnormal parenchymatous cells described. In the dry/non-dry front area, some of these abnormalities were also present but in small amount. Arranged in radial files, the cells of the second kind belonged to the secondary phloem parenchyma.

Primary walls of all the cell types were variously altered. The most frequent changes were higher osmiophily (Fig. 5*a*, *b*, *g*, *i–l*, *o*), degradation (Fig. 5*f*, *s*), generally starting from the middle lamella and external faces of primary walls, and accumulation of osmiophilic materials in the intercellular spaces (Fig. 5*g*, *p*, *r*, *s*). In the dry/non-dry front area, extremely high osmiophily was frequently observed in walls, but without degradation, and was associated with strong osmiophily of the lipid globules and electron-density of the entire cytoplasm.

Discussion

Tapping panel phloem of healthy rubber trees of the present study had the same histology as secondary phloem from barks and heveas of varied origin (Hébant and de Faÿ 1980; de Faÿ 1981; Hao and Wu 2000; Sando *et al*. 2009). At the ultrastructural level, the tapping panel phloem of mature rubber trees had been little investigated up to now and was not considered as a whole (de Faÿ *et al.* 1989). In this paper, the fine structure of laticifers, sieve tubes and phloem parenchyma cells of the inner phloem is specified in healthy mature trees belonging to clones GT1 and PB 260. Some aspects are also observable on micrographs taken from healthy material of varied origin: tapping panels from GT1 and some other clones (de Faÿ *et al.* 1989), young stems or branchlets from clone RRIM 600 (Wu and Hao 1990; Tian *et al.* 1998). They are, on the one hand, tight rubber globules within laticifers, and parenchyma cells having electron-dense or electron-lucent cytoplasm (de Faÿ *et al.* 1989); on the other hand, P-protein around sieve plate pores of a mature sieve element (Wu and Hao 1990) and common phloem parenchyma cells and companion cells of the type 'clear cells' (Tian *et al*. 1998). This suggests that the features described are essentially related to the cell types or the species. However, the amount of companion cells at an advanced stage of development associated with non-collapsed sieve elements and the marked differences between axial and radial phloem parenchyma cells ('clear' and 'dark' cells, respectively), could be related to age of the organ and/or to tapping. Indeed, early degradation of companion cells (for instance showing osmiophilic material in cavities close to the plasmalemma and broken nuclear envelope) was presumably connected to normal aging of the cells because these features have not been found in the young stem of 1-year-old heveas (E. de Faÿ, unpubl. data). Axial parenchyma cells of tapping panels are mainly laticifer sheath cells and, in the conducting phloem, common phloem parenchyma cells plus protein-storing cells (Wu and Hao 1987). Therefore, axial parenchyma cells are probably the most highly stressed by tapping. Difference in ultrastructure of axial and radial phloem parenchyma cells of the tapping panel might be exacerbated in regularly tapped rubber trees.

TPN is identical to irreversible TPD or a variant

In situ coagulation of latex, appearance of new cells that proliferate regularly or anarchically and increase of polyphenols (tannins and lignified secreted material) are phenomena characteristics of TPN. All the kinds of abnormalities detected by light microscopy in TPN-affected trees have already been described in TPD-affected heveas (de Faÿ and Hébant 1980; de Faÿ 1981; de Faÿ and Jacob 1989). Moreover, tylosoids – or the hyperplasic cells that derived from them – and the associated *in situ* coagulated latex were always present in TPN-affected phloem and are considered as the early structural markers of TPD (de Faÿ 1981; de Faÿ and Jacob 1989). There is thus histological evidence of a similarity between TPN and irreversible TPD. The similarity is supported by other facts: the impaired cyanide metabolism in TPN-affected rubber trees (Chrestin *et al*. 2004), and the cyanide-induction of tylosoids associated with *in situ* coagulated latex (de Faÿ *et al.* 2010).

Besides, the microscopic abnormalities did account for macroscopic symptoms of TPN-affected trees, as well as of TPD-affected ones. Progressive invasion of laticifers by tylosoids and/or 'gums', and *in situ* coagulation of latex logically result in bark dryness, which is a common symptom of TPN (Nandris *et al*. 1991) and TPD (Rands 1921; de Faÿ 1981; de Faÿ and Jacob 1989). The increase in oxidised phenolic compounds – tannins in some parenchyma cells and special lignins at the level of the golden yellow 'gums' – presumably leads to browning of bark. This was described as brown sheets and necrotic patches in TPN (Nandris *et al*. 1991) and golden specks or brown layer and dark brown areas in TPD (Petch 1921; Rands 1921; de Faÿ 1981; de Faÿ and Jacob 1989). The functioning of additional meristematic layers and of the cambium presumably explains the external symptoms. These were described as peripheral necrotic patches in TPN (Nandris *et al.*

1991) and bark cracking and flaking in both TPN (Nandris *et al*. 1991) and TPD (Petch 1921; Rands 1921; de Faÿ 1981; de Faÿ and Jacob 1989). The role of additional meristematic layers is to surround and isolate areas of necrotic tissues. As for the large ones of the phellogen type, it is to eliminate the whole outermost disorganised and necrotic tissue, which is clearly at the origin of bark cracking and flaking (de Faÿ 1981; de Faÿ and Jacob 1989). The cambium is known to push away the old tissue outwards, which presumably leads to make the disorganised and necrotic tissues visible. It is suggested that the macroscopic symptoms of TPN- and TPD-affected trees are connected with only small differences. These ones might be linked to differences in the descriptive approach of heveas.

However, depending on the affected clones, the environmental conditions or the stresses experienced by the trees, the phloem disorder might start at different places of the trees (base of the trunk typical of TPN; in relation with the tapping cut as usual in TPD). It might also develop more or less rapidly or in different manners (more specifically in extensive brown sheets and external necrotic patches for TPN, Nandris *et al*. 1991; in spectacular bark cracking and flaking or, sometimes, in trunk deforming for TPD, de Faÿ 1981). TPN and irreversible TPD might thus be two final aspects of the same syndrome. In conclusion, TPN is either identical to, or a variant of the irreversible form of TPD. Anyway, even if the origins of TPN and TPD were different, the same cellular reactions allow discussing the onset of cellular disorders within the tapping panel inner phloem.

Cellular degradation and dedifferentiation occur in the inner phloem of rubber tree tapping panels with the spread of the syndrome

TEM has revealed very numerous subcellular morphologic abnormalities in all the cell types of the tapping panel phloem of diseased trees. Those are related either to cellular degradation or cellular dedifferentiation. In the specialised cell elements forming laticiferous vessels and sieve tubes, the most characteristic change was the deposition of very osmiophilic materials. Indeed, these materials were absent in healthy barks, including in aging elements such as crushed sieve elements. Their presence relatively close to the cambium and in the dry/non-dry front area of tapping panels suggests an early appearance in the protoplasm of non-collapsed sieve elements and in that of laticifers where rubber particles were not yet fused. This indicates that these specialised cells were undergoing cell death of a form different from that of aging elements (at least for the sieve tubes). Furthermore, the formation of osmiophilic material in laticifers might be more specific to the syndrome than the fusion of rubber particles. In fact, exceptionally in barks of the healthy trees studied, a few rubber particles could be fused *in situ* very locally while the osmiophilic material was absent in the laticifer (data not shown). The osmiophilic materials of laticifers and sieve elements could be rich in unsaturated fatty acids since only the unsaturated fatty acids are intensively stained by osmium (Adams 1960). They could also contain proteins closely related to those forming a network at the far end of wounded laticifers when the flow of latex stops after the tapping of heveas, network which is precisely at the origin of the wound plugs (Hao *et al*. 2002). Wound lignins (phloroglucinol-HCl positive material) should then incrust such a matrix and the whole would form the ‘gums’. The non-osmiophilic masses deposited onto the sieve element walls common with the companion cells in non-crushed sieve tubes resemble callose. Callose is known to be a common wall constituent in sieve areas and to develop rapidly in reaction to injury. The amount and frequent location of this material out of the sieve plates in the TPN-affected trees suggest that the sieve tubes were strongly injured but not mechanically. Furthermore, the cytological signs of sieve element degradation and decompartmentation in the TPN-affected trees were consistent with the early disappearance of conducting sieve elements in TPD-sensitive rubber clones following cyanogenic treatments (de Faÿ *et al*. 2010).

Most of the other abnormalities were relevant either to cellular dedifferentiation or to cellular degradation. On the one hand, the abundance of big lipid or lipid-like globules and of ribosomes, the large amount of organelles specially mitochondria, as well as their division-like figures and irregular shapes, the arrangement of rough ER in extensive parallel arrays, and the presence of disproportionate large nuclei with big nucleoli were also reported in plant tumours (Ames 1972; Burgess and Fleming 1973; Camp and Whittingham 1974; Walne *et al*. 1975) or hyperplasic phloem (Esau and Hoefert 1978). The phenomena are considered as signs of cellular dedifferentiation. In the phloem of TPN-affected trees, those features were all found in the neighbourhood of laticifers having *in situ* coagulated latex, i.e. in tylosoids, hyperplasic cells, and additional meristematic and derived cells. The situation is comparable to that reported in naturally occurring tumour of a *Nicotiana* hybrid since the first sign of the tumour formation is the ‘activation’ of some cells adjacent to dead or dying cells (Brieger and Forster 1942). On the other hand, breaking up or disintegration of the membrane systems (plasma membranes, tonoplasts, outer membranes of organelles), alteration of plasmodesmata, formation of ER-derived structures and other vesicles containing cytoplasm, organelles or degraded materials, but also alterations of nuclear chromatin and walls were classic signs of cellular degradation and cell decompartmentation. Those abnormalities, all found in the phloem parenchyma cells and particularly in the axial ones, indicate that the cells were undergoing cell death.

Since signs of cellular dedifferentiation and degradation were found both in the same slivers (generally in different phloem layers and phloem cells, but sometimes in the same cells), in no way the cellular degradation can be taken for an artefact of handling or preparation of the specimen. Dedifferentiation and degradation were likely two reactions of the phloem parenchyma cells, either two different cellular behaviour or two stages in life cycle of the affected cells. Furthermore, the reaction of the parenchyma cells varied according to the position of the cells in the phloem (signs of dedifferentiation were always found in areas where latex was coagulated *in situ*, generally not very close to the conducting phloem, and mainly in axial cells). Cellular dedifferentiation that resulted in proliferation might be interpreted as an adaptative reaction of certain parenchyma cells to unfavourable conditions, as the presence of organelles having digitated form is interpreted in other parenchyma cells as evidence of an adaptative reaction to anaerobiose (Vartapetian

et al. 2003). But since a few parenchyma cells presented both features of dedifferentiation and degradation, it is likely that all the (axial?) phloem parenchyma cells went finally through cell death. Moreover, high osmiophily of lipids or lipid-like globules and cell walls, and absence of tonoplast were also found in cells not much altered otherwise, particularly in the dry/non-dry front area. These events would thus occur at early stage. It is finally suggested that the following phenomena: (i) high osmiophily and disintegration of the tonoplast in cells not much altered otherwise, (ii) cellular dedifferentiation and cell proliferation, and (iii) cellular degradation leading to cell decompartmentation would correspond in rubber trees to different stages of a stress reaction of the phloem parenchyma cells. The stress reaction would vary depending on whether the phloem cells were specialised or non-specialised since laticifers and sieve elements displayed a form of cell death different from that of parenchyma cells.

The changes in tapping panel phloem parenchyma cells are reminiscent of plant responses to stress, programmed cell death (PCD) or tumourigenesis and could be related to the up- or downregulated expression of genes associated with the onset of TPD and to impaired cyanide metabolism.

Early breaking up or disintegration of the membranes and appearance of tannin-like very electron-opaque material in the tapping panel phloem of diseased trees could indicate oxidative stress at the onset of phloem degeneration. Indeed, lipid peroxidation is known to be manifested by membrane alterations, notably by local and progressive breakages (Pasquali-Ronchetti *et al*. 1980), and tannins are considered as antioxidants (Amarowicz 2007). Moreover, these ultrastructural changes were in accordance with the biochemical evidence of polyphenol accumulation, increasing polyphenol oxidase activity and decreasing peroxidase activity in the barks of TPD-affected trees (Krishnakumar *et al*. 2001). Interestingly, some of the morphologic abnormalities observed in plastids and mitochondria of the phloem parenchyma cells were also reported in mitochondria of plants subjected to hypoxic or anoxic stresses (Vartapetian *et al*. 2003). The disappearance of the outer membrane of mitochondria was shown to occur in glucose-deprived conditions, and their disproportionate size and digitated shape to occur in presence of a source of sugars or an electron acceptor; the latter phenomena are regarded as adaptation to anaerobiose. Moreover, elongation, constriction and digitated shape of mitochondria were reported in cells of the spadice of *Sauromatum guttatum* during anthesis when thermogenesis takes place (Skubatz *et al*. 1993). Amiboid shape of plastids was reported in plant genetic tumours (Burgess and Fleming 1973).

About the forms of cell death associated with TPD, one may first think of necrosis, which is unnatural death of cells. However, many morphologic abnormalities described here also resemble features of several forms of PCD in plants. For instance, the large cisternae of rough ER coiling round cytoplasm and organelles, and the ER-derived vesicles are reminiscent of the concentric rings of ER sequestering cytoplasm and/or organelles found in aborting ovules during salt stress-induced abortion (Hauser *et al*. 2006), as well as in roots of seedlings subjected to sudden flooding (Gladish *et al*. 2006). An early disintegration of the tonoplast also occurred in maize roots during formation of aerenchyma (Campbell and Drew 1983). Very osmiophilic lipid-like globules have already been described in maize roots subjected to oxygen shortage during the formation of aerenchyma (Campbell and Drew 1983) and in the transitory floral nectary of *Digitalis purpurea* (Gaffal *et al*. 2007). Moreover, according to Campbell and Drew (1983), the dense cytoplasm and organelles likely indicate an early stage in development of these cells. Cell wall deterioration of the phloem was previously observed, accompanied by cellulose degradation, in TPN-affected trees (Nicole *et al*. 1991, 1992) and was reported in maize roots during the formation of aerenchyma (Campbell and Drew 1983; He *et al*. 1996).

Was the underlying process of cellular dedifferentiation and proliferation occurring in the parenchyma cells associated with altered laticifers true hyperplasia or neoplasia? Neoplasia is conceivable because, first, the growth of the cells exceeded and was uncoordinated with that of the normal secondary phloem around it; second, the cells did no longer resemble normal cells microscopically: they notably exhibited ultrastructural abnormalities already found in plant tumours as previously mentioned.

Several structural abnormalities observed in the inner phloem of TPN-affected trees might also be related to the genes up- or downregulated in the latex or bark of TPD affected-trees (Chen *et al*. 2002; Venkatachalam *et al*. 2007, 2009; Li *et al*. 2010). Notably, the disintegration of outer mitochondrial membranes in the trunk inner phloem of TPN-affected trees could be directly related to the *HbTOM20* gene (*Hevea brasiliensis T*ranslocase of the *O*uter *M*itochondrial *M*embrane) expression significantly downregulated in inner barks of TPD-affected trees compared with healthy one (Venkatachalam *et al*. 2009). Interestingly, systematic analyses of genes related to TPD suggest that the production and scavenging of reactive oxygen species and programmed cell death might play important roles in TPD (Li *et al*. 2010).

Cyanide is the mean of chemical defence against the outside attacks that is the most widely used in plants (over 3000 species of higher plants). In hevea, cyanogenesis was initially studied by Lieberei *et al*. (1985), and Moraes *et al*. (2002). As previously mentioned, de Faÿ *et al*. (2010) demonstrated that it was possible to induce the tylosoids associated with *in situ* coagulated latex in rubber tree by cyanogenic treatments. Taken together the present and previous results imply that cyanide induces dedifferentiation of axial parenchyma cells and cell death of the adjacent laticifers, and also leads to proliferation of dedifferentiated cells (since tylosoids give rise to hyperplasic cells). Furthermore, the literature shows that cyanide triggers PCD in cells of cowpea leaves (Ryerson and Heath 1996) and guard cells of pea leaves (Bakeeva *et al*. 2005; Dzyubinskaya *et al*. 2006). Ultimately, the abnormalities typical of the early disease syndrome could be caused by a stress related to impaired cyanide metabolism.

Conclusions and forward look

The distinction between the irreversible form of TPD (brown bast) and TPN (trunk panel necrosis) cannot be really supported. In the disease syndrome that causes reduction of the world rubber production, all cell types of the tapping panel phloem are affected

(not only the laticifers), and signs of cellular deterioration, dedifferentiation and proliferation are present from the outset. The irreversible TPD is considered as a degenerative disease of rubber tree having some similarities with plant response to stress, programmed cell death and tumourigenesis. Future works aimed at a better understanding of the causes and cellular mechanisms of TPD will have to specify the exact nature of the stress experienced by the rubber trees, notably in investigating the long-term effects of cyanogenic treatments, and the form(s) of cell death occurring with the phloem disorder or following cyanogenic treatments. Specify whether the proliferation persists in the same manner even after cessation of the original stimulus (such as cyanide induction), as in neoplasia, will also have to be a research objective. An exhaustive ultrastructural study appears to be an interesting complementary approach to molecular studies on TPD. The findings also provide new information on the biology of phloem (the trunk secondary phloem of mature trees was little studied up to now despite its role in tree nutrition) and on the plant disease syndromes (the physiological disease presently investigated has an unusual cellular phenotype).

Acknowledgements

This work was undertaken at the request of Dr Daniel Nandris and Dr Hervé Chrestin from the Institut de Recherche pour le Développement (IRD), Montpellier, France. It was in part financially supported by the French Institute of Rubber (IFC) and the group of hevea planters: Michelin (Clermond-Ferrand France), Socfinco (Bruxelles) and SIPH (Société Internationale de Plantation d'Hévéas). I thank Dr Michel Nicole (IRD) for giving some specimens to examine and Dr Nandris for providing the plant material from the Ivory Coast and organising the mission in the GREL plantation, Ghana.

References

Adams CWM (1960) Osmium tetroxide and the Marchi method: reactions with polar and non-polar lipids protein and polysaccharide. *The Journal of Histochemistry and Cytochemistry* **8**, 262–267. doi:10.1177/8.4.262

Amarowicz R (2007) Tannins: the new natural antioxidants? *European Journal of Lipid Science and Technology* **109**, 549–551. doi:10.1002/ejlt.200700145

Ames IH (1972) The fine structure of genetic tumor cells. *American Journal of Botany* **59**, 341–345. doi:10.2307/2441542

Bakeeva LE, Dzyubinskaya EV, Samuilov VD (2005) Programmed cell death in plants: ultrastructural changes in pea guard cells. *Biochemistry* **70**, 972–979. doi:10.1007/s10541-005-0211-3[Moscow]

Bobilioff W (1919) The cause of brown bast disease of *Hevea brasiliensis*. *Archief voor de Rubbercultuur in Nederlandsch-Indie* **3**, 172–178.

Brieger FG, Forster R (1942) Tumors in some hybrids of the genus *Nicotiana* – Tumores em certos hibridos do gênero *Nicotiana*. *Bragantia* **2**, 259–274. doi:10.1590/S0006-87051942000700002

Burgess J, Fleming EN (1973) The structure and development of a genetic tumour of the pea. *Protoplasma* **76**, 315–325. doi:10.1007/BF01279129

Camp RR, Whittingham WF (1974) Ultrastructural alterations in oak leaves parasitized by *Taphrina caerulescens*. *American Journal of Botany* **61**, 964–972. doi:10.2307/2441987

Campbell R, Drew MC (1983) Electron microscopy of gas space (aerenchyma) formation in adventitious roots of *Zea mays* L. subjected to oxygen shortage. *Planta* **157**, 350–357. doi:10.1007/BF00397407

Chen S, Peng S, Huang G, Wu K, Fu X, Chen Z (2002) Association of decreased expression of a Myb transcription factor with the TPD (tapping panel dryness) syndrome in *Hevea brasiliensis*. *Plant Molecular Biology* **51**, 51–58. doi:10.1023/A:1020719420867

Chrestin H, Sookmark U, Trouslot P, Pellegrin F, Nandris D (2004) Rubber tree (*Hevea brasiliensis*) bark necrosis syndrome: III. A physiological disease linked to impaired cyanide metabolism. *Plant Disease* **88**, 1047. doi:10.1094/PDIS.2004.88.9.1047B

Clément-Demange A, Priyadarshan PM, Hoa TTT, Venkatachalam P (2007) Hevea rubber breeding and genetics. *Plant Breeding Reviews* **29**, 177–283. doi:10.1002/9780470168035.ch4

Dzyubinskaya EV, Kiselevsky DB, Bakeeva LE, Samuilov VD (2006) Programmed cell death in plants: effect of protein synthesis inhibitors and structural changes in pea guard cells. *Biochemistry* **71**, 395–405. doi:10.1134/S0006297906040079[Moscow]

Esau K, Hoefert LL (1978) Hyperplastic phloem in sugar beetleaves infected with the beet curly top virus. *American Journal of Botany* **65**, 772–783. doi:10.2307/2442153

de Faÿ E (1981) Histophysiologie comparée des écorces saines et pathologiques (maladie des encoches sèches) de l'*Hevea brasiliensis*. PhD thesis, Université des Sciences et Techniques du Languedoc, Montpellier, France.

de Faÿ E, Hébant C (1980) Etude histologique des écorces d'*Hevea brasiliensis* atteint de la maladie des encoches sèches. *Comptes Rendus de l'Académie des Sciences, Paris, Série D* **291**, 865–868.

de Faÿ E, Jacob J-L (1989) The Bark Dryness disease (Brown Bast) of *Hevea*. Symptomatology, histological and cytological aspects. In 'Physiology of Rubber tree latex'. (Eds J d'Auzac, J-L Jacob, H Chrestin) pp. 407–430. (CRC Press Inc.: Boca Raton, FL)

de Faÿ E, Sanier C, Hébant C (1989) The distribution of plasmodesmata in the phloem of *Hevea brasiliensis* in relation to laticifer loading. *Protoplasma* **149**, 155–162. doi:10.1007/BF01322987

de Faÿ E, Moraes LAC, Moraes VH de F (2010) Cyanogenesis and the onset of tapping panel dryness in rubber tree. *Pesquisa Agropecuária Brasileira, Brasília* **45**, 1372–1380. doi:10.1590/S0100-204X2010001200006

Gaffal KP, Friedrichs GJ, El-Gammal S (2007) Ultrastructural evidence for a dual function of the phloem and programmed cell death in the floral nectary of *Digitalis purpurea*. *Annals of Botany* **99**, 593–607. doi:10.1093/aob/mcm002

Gladish DK, Xu J, Niki T (2006) Apoptosis-like programmed cell death in procambium and ground meristem of pea (*Pisum sativum*) root tips exposed to sudden flooding. *Annals of Botany* **97**, 895–902. doi:10.1093/aob/mcl040

Hao B-Z, Wu J-L (2000) Laticifer differentiation in *Hevea brasiliensis*: induction by exogenous jasmonic acid and linolenic acid. *Annals of Botany* **85**, 37–43. doi:10.1006/anbo.1999.0995

Hao B-Z, Wu J-L, Meng C-X, Gao Z-Q, Tan H-Y (2002) Laticifer wound plugging in *Hevea brasiliensis*: the role of a protein-network with rubber particle aggregations in stopping latex flow and protecting wounded laticifers. *Journal of Rubber Research* **7**, 281–299.

Hauser BA, Sun K, Oppenheimer DG, Sage TL (2006) Changes in mitochondrial membrane potential and accumulation of reactive oxygen species precede ultrastructural changes during ovule abortion. *Planta* **223**, 492–499. doi:10.1007/s00425-005-0107-x

Hébant C, de Faÿ E (1980) Functional organization of the bark of *Hevea brasiliensis* (Rubber tree): a structural and histoenzymological study. *Zeitschrift für Pflanzenphysiologie* **97**, 391–398.

He C-J, Morgan PW, Drew MC (1996) Transduction of an ethylene signal is required for cell death and lysis in the root cortex of maize during aerenchyma formation induced by hypoxia. *Plant Physiology* **112**, 463–472. doi:10.1104/pp.112.2.463

Jacob J-L, Prévôt J-C, Lacrotte R (1994) Tapping panel dryness in *Hevea brasiliensis* – L'encoche sèche chez *Hevea brasiliensis*. *Plantations Recherche Développement* **1**, 15–24.

Krishnakumar R, Annamalainathan K, Simon SP, Jacob J (2001) Tapping panel dryness syndrome in *Hevea* increases dark respiration but not ATP status. *Indian Journal of Natural Rubber Research* **14**, 14–19.

Lieberei R, Selmar D, Biehl B (1985) Metabolization of cyanogenic glucosides in *Hevea brasiliensis*. *Plant Systematics and Evolution* **150**, 49–63. doi:10.1007/BF00985567

Li D, Deng Z, Chen C, Xia Z, Wu M, He P, Chen S (2010) Identification and characterization of genes associated with tapping panel dryness from *Hevea brasiliensis* latex using suppression substractive hybridization. *BMC Plant Biology* **10**, 140–152. doi:10.1186/1471-2229-10-140

Moraes LAC, Moraes VH de F, Moreira A (2002) Effect of the cyanogenesis on the incompatibility of crown clones of *Hevea spp.* budded onto IPA 1 – Efeito da cianogênese na incompatibilidade entre clones de copa de seringueira e o clone de painel IPA 1. *Pesquisa Agropecuária Brasileira* **37**, 925–932. doi:10.1590/S0100-204X2002000700005

Nandris D, Chrestin H, Noirot M, Nicole M, Thouvenel JC, Geiger JP (1991) La nécrose du phloème du tronc de l'Hévéa en Côte d'Ivoire: I. Symptomatologie et caractéristiques biochimiques. *European Journal of Forest Pathology* **21**, 325–339. doi:10.1111/j.1439-0329.1991.tb00771.x

Nandris D, Moreau R, Pellegrin F, Chrestin H, Abina J, Angui P (2004) Rubber tree (*Hevea brasiliensis*) bark necrosis syndrome: II. First comprehensive report on causal stresses. *Plant Disease* **88**, 1047. doi:10.1094/PDIS.2004.88.9.1047A

Nicole M, Thouvenel JC, Giannotti J, Chrestin H, Geiger JP, Nandris D, Rio B (1991) The histology of *Hevea brasiliensis* phloem necrosis. *European Journal of Forest Pathology* **21**, 27–35. doi:10.1111/j.1439-0329.1991.tb00299.x

Nicole M, Chamberland H, Nandris D, Ouellette GB (1992) Cellulose is degraded during phloem necrosis of *Hevea brasiliensis*. *European Journal of Forest Pathology* **22**, 266–277. doi:10.1111/j.1439-0329.1992.tb00793.x

Pasquali-Ronchetti I, Bini A, Botti B, De Alojsio G, Fornieri C, Vannini V (1980) Ultrastructural and biochemical changes induced by progressive lipid peroxidation on isolated microsomes and rat liver endoplasmic reticulum. *Laboratory Investigation* **42**, 457–468.

Petch T (1921) 'The diseases and pests of the Rubber tree'. (Macmillan and Co: London)

Rands RD (1921) Brown Bast disease of plantation rubber; its cause and prevention. *Archief voor de Rubbercultuur in Nederlandsch-Indie* **5**, 223–278.

Ryerson DE, Heath MC (1996) Cleavage of nuclear DNA into oligonucleosomal fragments during cell death induced by fungal infection or by abiotic treatments. *The Plant Cell* **8**, 393–402. doi:10.1105/tpc.8.3.393

Sando T, Hayashi T, Takeda T, Akiyama Y, Nakazawa Y, Fukusaki E, Kobayashi A (2009) Histochemical study of detailed laticifer structure and rubber biosynthesis-related protein localization in *Hevea brasiliensis* using spectral confocal laser scanning microscopy. *Planta* **230**, 215–225. doi:10.1007/s00425-009-0936-0

Sass JE (1958) 'Botanical microtechnique'. 3rd edn. (The Iowa State College Press: Ames, IA)

Skubatz H, Kunkel DD, Meeuse BJD (1993) Ultrastructural changes in the appendix of the *Sauromatum guttatum* inflorescence during anthesis. *Sexual Plant Reproduction* **6**, 153–170. doi:10.1007/BF00228644

Tian W-M, Han Y-Q, Wu J-L, Hao B-Z (1998) Characteristics of protein-storing cells associated with a 67 kDa protein in *Hevea brasiliensis*. *Trees (Berlin)* **12**, 153–159. doi:10.1007/PL00009705

Vallet C, Chabbert B, Czaninski Y, Montiès B (1996) Histochemistry of lignin deposition during sclerenchyma differentiation in alfalfa stems. *Annals of Botany* **78**, 625–632. doi:10.1006/anbo.1996.0170

Vartapetian BB, Andreeva IN, Generozova IP, Polyakova LI, Maslova IP, Dolgikh YI, Stepanova AY (2003) Functional electron microscopy in studies of plant responses and adaptation to anaerobic stress. *Annals of Botany* **91**, 155–172. doi:10.1093/aob/mcf244

Venkatachalam P, Thulaseedharan A, Raghothama K (2007) Identification of expression profiles of tapping panel dryness (TPD) associated genes from the latex of rubber tree (*Hevea brasiliensis* Muell. Arg.). *Planta* **226**, 499–515. doi:10.1007/s00425-007-0500-8

Venkatachalam P, Thulaseedharan A, Raghothama K (2009) Molecular identification and characterization of a gene associated with the onset of tapping panel dryness (TPD) syndrome in rubber tree (*Hevea brasiliensis* Muell.) by mRNA differential display. *Molecular Biotechnology* **41**, 42–52. doi:10.1007/s12033-008-9095-y

Walne PL, Haber AH, Triplett LL (1975) Ultrastructure of auxin-induced tumors of the coleorhiza-epiblast of wheat. *American Journal of Botany* **62**, 58–66. doi:10.2307/2442078

Wu J-L, Hao B-Z (1987) Ultrastructure and differentiation of protein-storing cells in secondary phloem of *Hevea brasiliensis*. *Annals of Botany* **60**, 505–512.

Wu J-L, Hao B-Z (1990) Ultrastructure of P-protein in *Hevea brasiliensis* during sieve-tube development and after wounding. *Protoplasma* **153**, 186–192. doi:10.1007/BF01354003

Manuscript received 26 February 2011, accepted 25 July 2011